

**Anomalous variations in the volume of Fe<sub>69</sub>Ni<sub>31</sub> Invar alloys under high pressure and temperature**M. Matsushita,<sup>1,\*</sup> T. Inoue,<sup>2</sup> I. Yoshimi,<sup>2</sup> T. Kawamura,<sup>2</sup> Y. Kono,<sup>2</sup> T. Irifune,<sup>2</sup> T. Kikegawa,<sup>3</sup> and F. Ono<sup>4</sup><sup>1</sup>*Department of Mechanical Engineering, Graduate School of Science and Engineering, Ehime University, Bunkyo-cho 3, Matsuyama, Ehime 790-8577, Japan*<sup>2</sup>*Geodynamics Research Center, Ehime University, Bunkyo-cho 2-5, Matsuyama, Ehime 790-8577, Japan*<sup>3</sup>*Institute of Material Structure Science, High Energy Accelerator Research Organization, Tsukuba, Ibaraki 305-0801, Japan*<sup>4</sup>*Department of Physics, Faculty of Science, Okayama University, Tsushima-naka 3-1-1, Okayama 700-8530, Japan*

(Received 26 July 2007; revised manuscript received 15 November 2007; published 26 February 2008)

We have investigated the variations in the crystal structure of Fe<sub>69</sub>Ni<sub>31</sub> Invar alloys under high pressures below 6.5 GPa and high temperatures below 1300 K using energy dispersive x-ray diffraction. The crystal structure is stabilized as a face-centered-cubic (fcc) lattice structure over the entire investigated range. However, the volume of the fcc in Fe<sub>69</sub>Ni<sub>31</sub> shows an abrupt decrease at 1300 K above 2 GPa and at 1100 K above 3 GPa with increasing pressure. These results show that a pressure-induced phase transition to a low-volume state occurs under high-temperature and high-pressure conditions. We consider this transition would be that from the high-spin state to the low-spin state, which has been speculated in some previous theoretical studies.

DOI: [10.1103/PhysRevB.77.064429](https://doi.org/10.1103/PhysRevB.77.064429)

PACS number(s): 75.50.Bb

**I. INTRODUCTION**

In Invar alloys, below the Curie temperature ( $T_C$ ), the thermal expansion coefficients become very small. Fe-Ni alloys with a Ni concentration around 35% are the most common Invar alloys.<sup>1</sup> The characteristic features of Invar alloys are not only their small thermal expansion coefficients but also their large negative pressure dependence on the Curie temperature and magnetization.<sup>2</sup> Numerous studies have been performed since the discovery of the Invar effect; however, its mechanism has not been completely understood.

Studies on the volume and temperature dependence of the electronic and magnetic states of Invar alloys have been conducted by Weiss in 1963.<sup>3</sup> Weiss presented a model of the mechanism of the Invar effect, the so-called  $2\gamma$  model. Weiss assumed two different states in an Invar alloy: a high-volume state with a large magnetic moment and a low-volume state with a smaller magnetic moment. According to this model, the Invar effect is caused by the transition from the high-volume state to the low-volume state with increasing temperature and/or pressure.

Some theoretical studies on Invar alloys in the 1990s have provided new information.<sup>4–8</sup> The energy and volume differences between the low-spin (LS) and high-spin (HS) states of Invar alloys are very small. At ambient pressure, the HS acquires the ground state; however, the population of the LS increases with temperature and/or pressure. These studies suggest that the HS-LS transition is the origin of the Invar effect, which highlights the Weiss  $2\gamma$  model. On the other hand, some theoretical studies have shown that a noncollinear magnetic state assumes the lowest energy in the volume range between the HS and the LS.<sup>9,10</sup> In particular, Schilfgaard *et al.* have presented a new concept for the mechanism of the Invar effect.<sup>10</sup> Their model explains that the ferromagneticlike noncollinear magnetic phase assumes the ground state at ambient pressure and that the origin of the Invar effect is the anomalously small Grüneisen constant induced by the anomalously small volume-energy curve of the noncollinear magnetic state.

From the above-mentioned theoretical prediction, there is a possibility that two kinds of phase transitions—one of the electronic states and the other of the magnetic interactions—occur under finite temperature and pressure. Moreover, an investigation into the existence of the phase transition is important in understanding the mechanism of the Invar effect.

The pressure-induced magnetic state transition of Invar alloys has been reported by some experimental studies.<sup>11–16</sup> According to our previous studies on the magnetism of Invar alloys under high pressure, the ferromagnetic state collapses and spin-glass-like magnetic phases appear from the low-temperature side with increasing pressure.<sup>12–14</sup> Moreover, some experiments have reported that the local magnetic moments in Invar alloys decrease in two steps at room temperature with increasing pressure.<sup>15,16</sup> This pressure-induced transition observed at room temperature is not accompanied by a remarkable volume variation.<sup>15,16,18</sup> In addition, some groups have performed several experimental studies on the pressure variation of the volume and bulk modulus ( $B$ ) of Invar alloys.<sup>17–21</sup> Certain studies have reported that the  $B$  value of Invar alloys shows negative pressure dependence at room temperature.<sup>17–19</sup> These reports are in agreement with the theoretical prediction by Schilfgaard *et al.*<sup>10</sup> However, Decremps and Nataf reported that the  $B$  value of Fe<sub>64</sub>Ni<sub>36</sub> does not show a negative pressure dependence.<sup>20</sup> The pressure-induced variation in volume at low temperatures has been investigated by two groups.<sup>19,21</sup> They have reported that lattice softening occurs in Fe-Pt Invar alloys under high pressure above 4 GPa.

On the other hand, the number of studies on Invar alloys at high temperature and pressure is limited. Acet *et al.* reported that the Fe<sub>50</sub>Ni<sub>37</sub>Mn<sub>13</sub> ferromagnetic alloy shows a small Invar effect just below  $T_C$ . Further, it shows an anti-Invar effect above  $T_C$  at ambient pressure.<sup>22</sup> Dubrovinsky *et al.* reported the pressure-induced Invar effect in Fe-Ni alloys in a concentration apart from the Invar region, for example, Fe<sub>20</sub>Ni<sub>80</sub> alloy.

If the HS-LS transition predicted by theoretical studies would occur, the volume of the Invar alloy would drastically

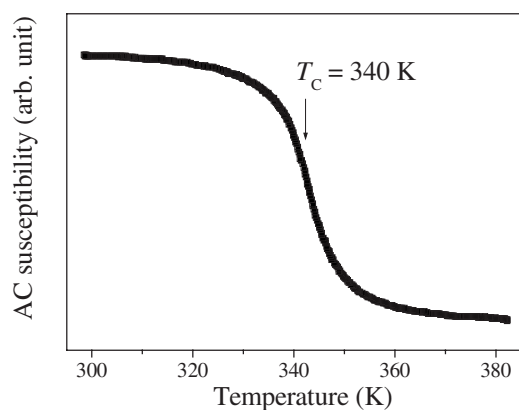


FIG. 1. Temperature dependence of ac susceptibility ( $\chi$ ).

decrease with increasing pressure. In addition, the HS-LS transition should occur at a high temperature. However, this type of transition has not yet been observed. Therefore, we note the pressure ( $P$ )–volume ( $V$ )–temperature ( $T$ ) relation for  $\text{Fe}_{69}\text{Ni}_{31}$  Invar alloy for the temperature range of 500–1300 K under high pressures of up to 6.5 GPa.

## II. EXPERIMENTAL METHOD

### A. Sample preparation

An Fe-Ni ingot was prepared by arc melting and was then annealed at 1273 K in an evacuated silica tube for 1 week, followed by quenching it into water. Subsequently, the sample was crushed into powder for x-ray diffraction measurements under high pressure. To remove the residual stress, the powdered sample was annealed again at 1273 K in an evacuated silica tube for 3 h and then quenched into water. The chemical composition was determined as  $\text{Fe}_{69}\text{Ni}_{31}$  using the Curie temperature ( $T_C=340$  K) that was denoted as the maximum slope of the alternating current (ac) susceptibility-temperature ( $\chi$ - $T$ ) curve and energy-dispersive x-ray spectroscopy (EDS). The observed  $\chi$ - $T$  curve is shown in Fig. 1. The chemical compositions obtained by  $T_C$  and EDS almost correspond with each other, and this result agrees with the previous report.<sup>2</sup> The face-centered-cubic lattice (fcc) crystal structure of the sample was confirmed by x-ray diffraction measurements.

### B. X-ray diffraction measurements under high pressure

X-ray diffraction measurements were performed by the energy-dispersive method using a synchrotron radiation beam on the AR-NE5C beam line at the photon factory of the High Energy Accelerator Research Organization in Japan. The incident white x-ray beam was reduced to  $0.2 \times 0.2 \text{ mm}^2$  using a pair of slits. The horizontal width of the collimator was 0.1 mm. The vertical and horizontal widths of the receiving slits were 0.2 and 0.3 mm, respectively. A Ge solid-state detector that was calibrated using the characteristic x-rays of Ag, Au, Bi, Cu, Dy, Mo, Pb, Pt, and Ta was used. The diffraction angle was fixed at  $6^\circ$  to cover the main diffraction peaks of the sample and pressure marker.

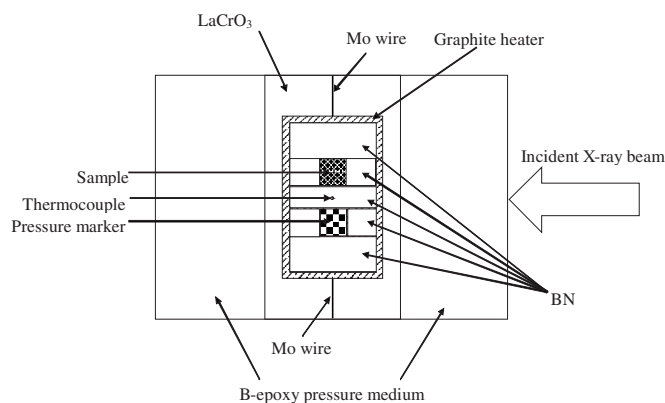


FIG. 2. A schematic illustration of the cross section of the high-pressure cell for the horizontal plain parallel to the incident x-ray beam.

The pressure was generated using a cubic anvil-type high-pressure apparatus installed at the AR-NE5C beam line. A cross section of the sample assembly in the horizontal plane parallel to the incident x-ray beam is shown in Fig. 2. Boron epoxy and graphite were used as the pressure-transmitting material and heater, respectively. Two BN capsules that were set symmetrically against the center of the high-pressure cell were filled with the sample and pressure marker, respectively. The pressure was determined from the unit cell volume of MgO using an equation of state proposed by Jamieson *et al.*<sup>23</sup> The temperature was determined using a  $\text{W}_{75}\text{Re}_{25}$ - $\text{W}_{97}\text{Re}_3$  thermocouple with a diameter of 0.1 mm. The distance between the  $\text{Fe}_{69}\text{Ni}_{31}$  alloy and the thermocouple was the same as that between MgO and the thermocouple.

In the present experiments, a load was first applied to the maximum target value, following which the temperature was increased up to 1300 K. The x-ray diffraction patterns of the pressure marker and  $\text{Fe}_{69}\text{Ni}_{31}$  alloy were collected only during the cooling process. Subsequently, the load was decreased to the target value, and then the process of collecting the x-ray diffraction patterns was repeated. The series of experiments was performed twice. One series was performed using tungsten-carbide (WC) anvils with the edge length of the front face being  $6 \times 6 \text{ mm}^2$  (hereinafter, we refer to this experiment series as run 1), mainly to obtain the pressure range data below approximately 3.5 GPa. Another series was performed using WC anvils with the front face being  $4 \times 4 \text{ mm}^2$  (hereinafter, we refer to this experiment series as run 2), mainly to obtain the high-pressure range data above approximately 3.5 GPa.

To obtain sharp x-ray diffraction patterns and a precise lattice constant of the sample and pressure marker, it is necessary to remove the pressure gradient and residual stress in the case of using a solid pressure medium. In the case of the present experiments, each applied load was required to be annealed at 1300 K. Therefore, we performed the x-ray diffraction measurements during the cooling process.

## III. RESULTS AND DISCUSSION

In this study, the volumes of  $\text{Fe}_{69}\text{Ni}_{31}$  were determined by using at least four of the five main x-ray diffraction peaks of

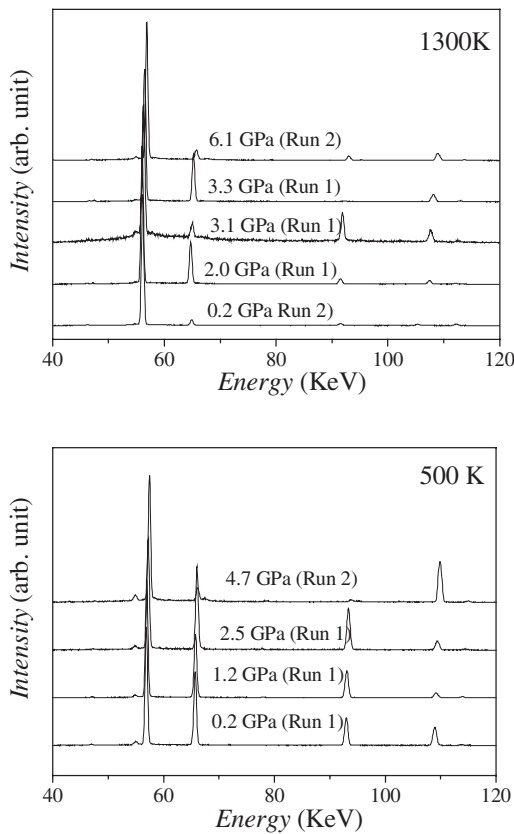


FIG. 3. Observed x-ray diffraction patterns at various pressures and temperatures.

$\text{Fe}_{69}\text{Ni}_{31}$ , for example, (111), (200), (220), (311), and (222). Some of the observed x-ray diffraction patterns are shown in Fig. 3. It can be observed that the crystal structure is stabilized on the fcc lattice over the entire measured range. The pressure was determined by the volumes of MgO using the state equation proposed by Jamieson *et al.*<sup>23</sup> The volume of MgO was determined by using at least four of the five main x-ray diffraction peaks of MgO, for example, (111), (200), (220), (311), and (222).

The observed pressure variations of the volume at various temperatures obtained in runs 1 and 2 are shown in Fig. 4. The volume was normalized to that at ambient pressure and room temperature. The curves shown in Fig. 4 are visual guides.

The pressure variation in the volume of  $\text{Fe}_{69}\text{Ni}_{31}$  at 1300 K is shown in Fig. 4(a). It is observed that the volume decreases drastically by approximately 4% between 2 and 4 GPa. From this result, it is considered that the pressure-induced phase transition to a low-volume state occurs above 2 GPa at 1300 K.

The pressure variation in the volume of  $\text{Fe}_{69}\text{Ni}_{31}$  at 1100 K is shown in Fig. 4(b). The volume drastically decreases by approximately 3% between 3 and 5 GPa. From this result, it is considered that the pressure-induced phase transition to a low-volume state occurs above 3 GPa at 1100 K.

On the other hand, the obvious abrupt pressure-induced decrease in volume is not observed in  $\text{Fe}_{69}\text{Ni}_{31}$  at 900, 700, and 500 K, which are shown in Figs. 4(c)–4(e), respectively.

These results indicate the existence of the pressure-induced transition with large volume variation at least at 1300 and 1100 K.

The visual guides in Fig. 4 were drawn according to the following procedure. Initially, we fitted all the data points at various temperatures using the following Boltzmann function:

$$V = (A_1 - A_2)/(1 + e^{(P-P_C)/W}) + A_2,$$

where  $A_1$ ,  $A_2$ ,  $P_C$ , and  $W$  are constants. We consider this function and method to be suitable for the searching of the pressure-induced transition of volume. However, this function cannot reflect the effect of compressibility of the high-volume state and the low-volume state, for example, at 1300 and 1100 K. The amount of data in the present experiments is sufficient to estimate the compressibility of the high-volume state; however, it cannot estimate the compressibility of the low-volume state. Thus, we fitted the data points at 1300 and 1100 K below 2 GPa using the following first-order linear function:

$$V = A \times P + V_0(T),$$

where  $A$  is a constant and  $V_0(T)$  is the extrapolated normalized volume at each temperature at ambient pressure. We draw the visual guide using the first-order linear function fit up to 2 and 3 GPa at 1300 and 1100 K, respectively. In addition to the above pressure range, we use the Boltzmann function fit as the visual guide.

Rueff *et al.* reported that the amplitude of the Fe local moment in  $\text{Fe}_{64}\text{Ni}_{36}$  is reduced at two characteristic step values with increasing pressure at 300 K.<sup>15</sup> In their report, this pressure dependence of the Fe local moment is interpreted in terms of transitions from a HS to a LS up to 5 GPa followed by a transition to a nonmagnetic state above 15 GPa. Dubrovinsky *et al.* reported the pressure variation of volume in  $\text{Fe}_{64}\text{Ni}_{36}$  under high pressure up to 20 GPa at room temperature.<sup>18</sup> However, it cannot be seen that the obviously discontinuous volume varies with the above-mentioned pressure-induced magnetic state transition. On the other hand, in the present study at 1300 and 1100 K, we confirm the discontinuous volume variation with increasing pressure. Therefore, we consider that the anomalous pressure variations of volume at 1300 and 1100 K indicate a pressure induced spin state transition, but it would be of a different type from that observed at room temperature.

The temperature dependence of the compressibility in  $\text{Fe}_{69}\text{Ni}_{31}$  below 2 GPa is shown in Fig. 5. The compressibility at various temperatures was estimated from the results of the first-order linear fit of the data from run 1 below 2 GPa. It can be observed that the compressibility decreases drastically above 900 K. The similar tendency is also confirmed from the data obtained from run 2.

The temperature dependencies of the normalized volume at various pressures up to 4 GPa obtained from the visual guides in Fig. 4 are shown in Fig. 6. At 3.0 GPa, the thermal expansion between 1100 and 1300 K is clearly lesser than that below 2.5 GPa. Moreover, above 3.5 GPa, the thermal expansion is less above 900 K. The shapes of  $T$ - $V$  curves above 3.0 GPa correspond well with the theoretical predic-

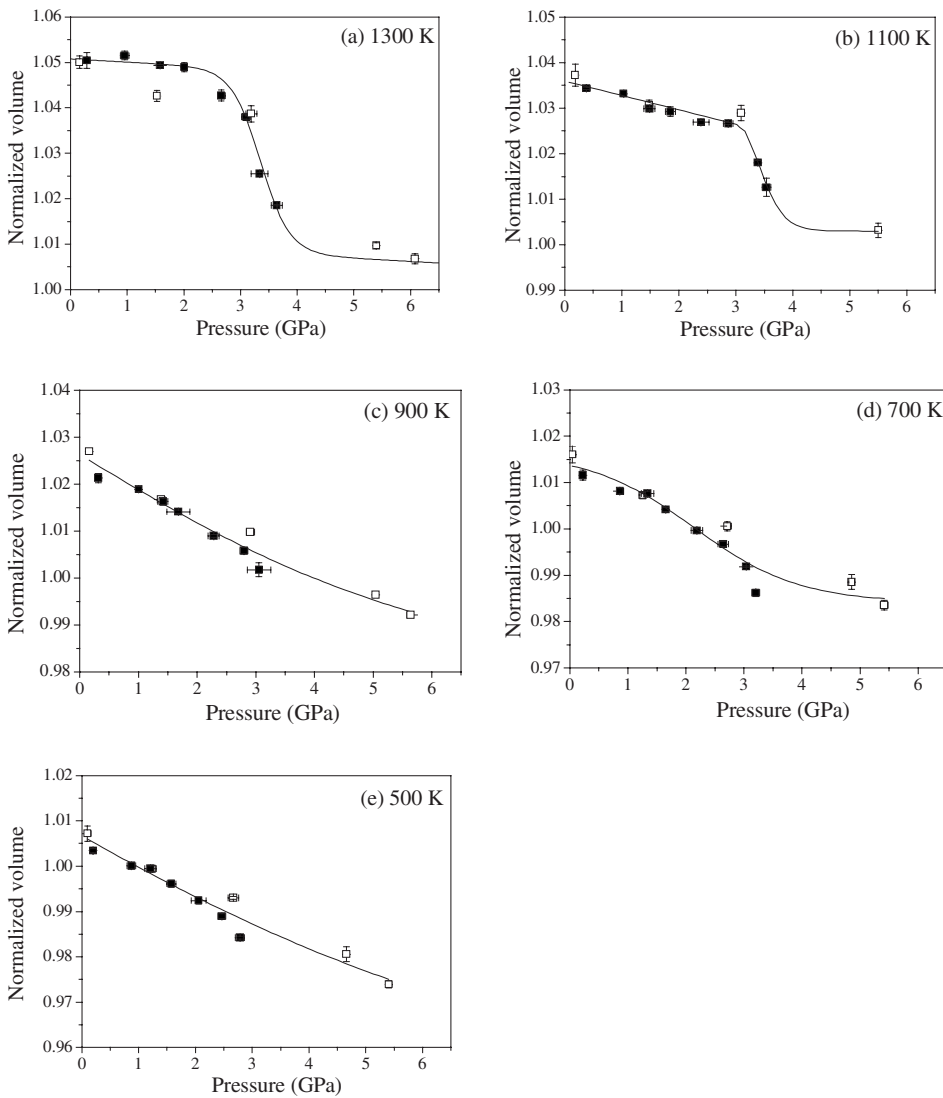


FIG. 4. Pressure dependences of the volume of  $\text{Fe}_{69}\text{Ni}_{31}$  at various temperatures. Each temperature is expressed in figures. The closed and open squares are the data obtained from runs 1 and 2, respectively. The curves in these figures are visual guides.

tion by Moruzzi with regard to the thermally induced HS-LS transition of the Invar alloy.<sup>4</sup> From these results, it would be considered that the decrease in the thermal expansion coefficients with increasing temperature above 900 K and 3.0 GPa is the Invar effect caused by the HS-LS transition.

Below 2 GPa, the thermal expansion increases with pressure, which corresponds to the pressure dependence of the

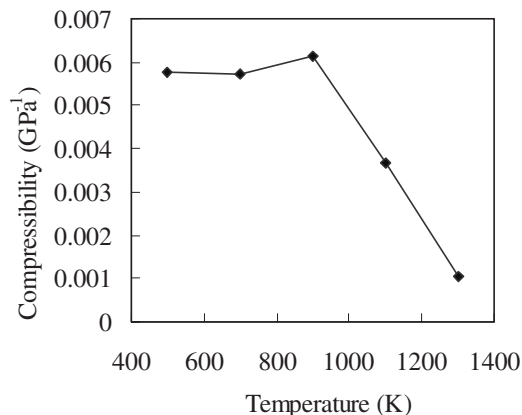


FIG. 5. Temperature dependence of compressibility.

above-mentioned compressibility. According to a previous ac susceptibility study under high pressure, the magnetic interaction changes from ferromagnetic to antiferromagnetic with increasing pressure.<sup>12</sup> According to the theoretical study by Herper *et al.*, the changes in the short-range magnetic inter-

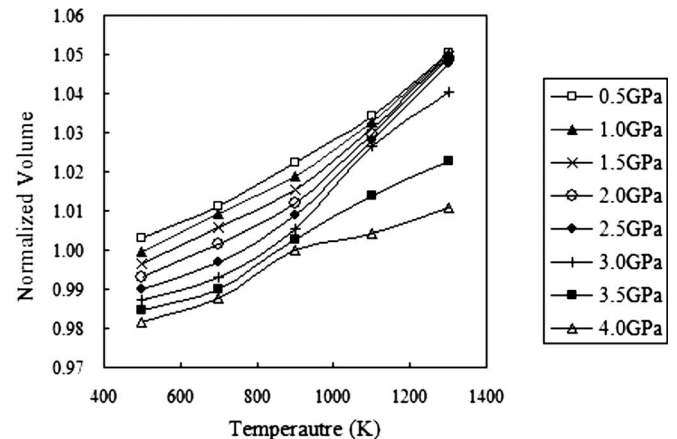


FIG. 6. Temperature dependence of volume at various pressures.



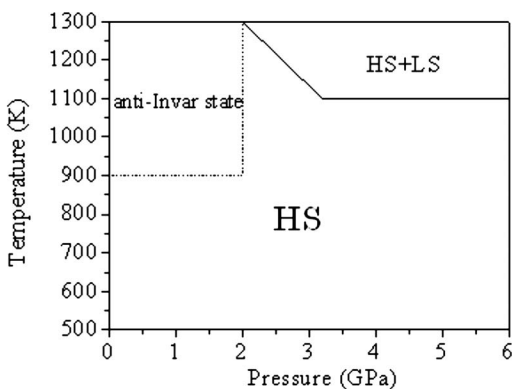


FIG. 7. The  $P$ - $T$  phase diagram obtained from the present experiments. HS and LS show high-spin state and low-spin state, respectively.

action cause the anti-Invar effect and anomalous bulk modulus variation.<sup>24</sup> We consider that the changes in the interaction among the nearest atoms could cause the thermal expansion and bulk modulus.

The  $P$ - $T$  phase diagram obtained by the present experiments is shown in Fig. 7. At 1300 and 1100 K, the transitions from the HS state to the low-volume state are initiated at 2 and 3 GPa, respectively. However, these transitions cannot be seen below 900 K in present experiments. Above 900 K and below 2 GPa, low compressibility and high thermal expansion state exist, as shown in Figs. 5 and 6. We

expressed this  $P$ - $T$  range as an anti-Invar state shown in Fig. 7.

After these high-pressure experiments, the composition of the sample was confirmed using EDS and x-ray diffraction measurements. The composition did not change, and no remarkable diffraction peaks of the reacted material were observed in the x-ray patterns.

#### IV. CONCLUSION

The  $P$ - $V$ - $T$  relation for  $\text{Fe}_{69}\text{Ni}_{31}$  was investigated at temperatures up to 1300 K and at pressures below 6.5 GPa. The following conclusions can be drawn from our present study.

(1) A pressure-induced discontinuous variation in volume has been observed in  $\text{Fe}_{69}\text{Ni}_{31}$  at 1300 K above 2 GPa and at 1100 K above 3 GPa. These results show that the pressure-induced transition to a low-volume state occurs at least at 1300 and 1100 K.

(2) Below 2 GPa and above 900 K, the compressibility decreases and the thermal expansion increases with pressure.

(3) The thermal expansion behavior between 3 and 4 GPa corresponds well with the theoretical calculation with regard to thermally induced HS-LS transition of the Invar alloy.<sup>4</sup>

#### ACKNOWLEDGMENTS

The authors wish to thank M. Katsuta for his help. We also thank the High-Energy Accelerator Research Organization (KEK) for the beam time throughout the Project No. 07G107.

\*Corresponding author; FAX: +81-89-927-9902; matsushita@eng.ehime-u.ac.jp

<sup>1</sup>Ch. E. Guillaume, C. R. Hebd. Seances Acad. Sci. **125**, 235 (1897).

<sup>2</sup>E. F. Wassermann, *Ferromagnetic Materials*, edited by K. H. J. Buschow and E. P. Wohlfarth (North-Holland, Amsterdam, 1990), Vol. 5, p. 238.

<sup>3</sup>R. J. Weiss, Proc. Phys. Soc. London **82**, 281 (1963).

<sup>4</sup>V. L. Moruzzi, Phys. Rev. B **41**, 6939 (1990).

<sup>5</sup>M. Podgorny, Phys. Rev. B **46**, 6293 (1992).

<sup>6</sup>P. Entel, E. Hoffmann, P. Mohn, K. Schwarz, and V. L. Moruzzi, Phys. Rev. B **47**, 8706 (1993).

<sup>7</sup>I. A. Abrikosov, O. Eriksson, P. Söderlind, H. L. Skriver, and B. Johansson, Phys. Rev. B **51**, 1058 (1995).

<sup>8</sup>R. Hayn and V. Drchal, Phys. Rev. B **58**, 4341 (1998).

<sup>9</sup>M. Uhl, L. M. Sandratskii, and J. Kubler, Phys. Rev. B **50**, 291 (1994).

<sup>10</sup>M. van Schilfgarde, I. A. Abrikosov, and B. Johansson, Nature (London) **400**, 46 (1999).

<sup>11</sup>M. M. Abd-Elmeguid and H. Micklitz, Phys. Rev. B **40**, 7395 (1989).

<sup>12</sup>M. Matsushita, S. Endo, K. Miura, and F. Ono, J. Magn. Magn. Mater. **265**, 352 (2003).

<sup>13</sup>M. Matsushita, S. Endo, K. Miura, and F. Ono, J. Magn. Magn. Mater. **269**, 393 (2004).

<sup>14</sup>M. Matsushita, Y. Miyoshi, S. Endo, and F. Ono, Phys. Rev. B

**72**, 214404 (2005).

<sup>15</sup>J. P. Rueff, A. Shukla, A. Kaprolat, M. Krisch, M. Lorenzen, F. Sette, and R. Verbeni, Phys. Rev. B **63**, 132409 (2001).

<sup>16</sup>S. Odin, F. Baudelet, J. P. Itié, A. Polian, S. Pizzini, A. Fontaine, Ch. Giorgetti, E. Prtyge, and J. P. Kappler, J. Appl. Phys. **83**, 7291 (1998).

<sup>17</sup>L. Mañosa, G. A. Saunders, H. Rahdi, U. Kawald, J. Pelzl, and H. Bach, Phys. Rev. B **45**, 2224 (1992).

<sup>18</sup>L. Dubrovinsky, N. Dubrovinskaia, I. A. Abrikosov, M. Vennström, F. Westman, S. Carlson, M. van Schilfgarde, and B. Johansson, Phys. Rev. Lett. **86**, 4851 (2001).

<sup>19</sup>M. Matsushita, Y. Nakamoto, E. Suzuki, Y. Miyoshi, H. Inoue, S. Endo, T. Kikegawa, and F. Ono, J. Magn. Magn. Mater. **284**, 403 (2004).

<sup>20</sup>F. Decremps and L. Nataf, Phys. Rev. Lett. **92**, 157204 (2004).

<sup>21</sup>L. Nataf, F. Decremps, M. Gauthier, and B. Canny, Phys. Rev. B **74**, 184422 (2006).

<sup>22</sup>M. Acet, H. Zähres, E. F. Wassermann, and W. Pepperhoff, Phys. Rev. B **49**, 6012 (1994).

<sup>23</sup>J. C. Jamieson, J. N. Fritz, and M. H. Manghnani, in *High-Pressure Research in Geophysics*, edited by S. Akimoto and M. H. Manghnani (Center for Academic Publishing, Tokyo, 1982), pp. 27–48.

<sup>24</sup>H. C. Herper, E. Hoffmann, and P. Entel, Phys. Rev. B **60**, 3839 (1999).